



Fusion Reactor Design

Vacuum Team

BY:

ELISA BUGLIONE-CERESA, TOBI GAGGL, VIKTORIA KEUSCH,
ELENA STEINWENDER, MARTIN TRITTHART, ELENA WALLNER

SUPERVISED BY:

ALBERT, CHRISTOPHER, ASS.PROF. DIPLO.-ING. DR.RER.NAT. BSc
SCHENNACH, ROBERT, Ao.UNIV.-PROF. MAG. DR.RER.NAT.

JULY 16, 2024

Contents

1 Design of the vacuum chamber	5
1.1 Main recipient	5
1.1.1 Flanges	6
1.1.2 Drill holes - options for installing windows and connections	6
1.1.3 FEM simulations for different lid designs	7
1.1.4 Finished design for the time being:	8
1.2 Ports and feedthrough	10
1.2.1 (Double) o-ring gasket	10
1.2.2 Copper gasket	10
1.2.3 Gas injection ports	11
1.2.4 Ventilation valves	12
1.2.5 Windows	13
1.2.6 Sealings	13
1.2.7 Current feedthrough	14
1.2.8 Coaxial feedthrough	15
1.2.9 Cooling liquid feedthrough	15
1.3 Manipulators (Mechanical feedthroughs)	15
1.3.1 Bellows	16
1.3.2 Manipulator for Langmuir probe	16
1.3.3 Pieco motor for the interferometer mirror	16
1.4 Overview of the ports of each team	17
1.4.1 Vacuum - Team	17
1.4.2 Coil - Team	18
1.4.3 Design - Team	18
1.4.4 Diagnostic - Team	19
1.4.5 Heating - Team	21
1.5 Conclusion	22
1.6 Outlook	22
2 Vacuum design	23
2.1 Pressure	23
2.2 Pumps	23
2.3 Vacuum analysis	24
2.3.1 Pressure measurement	24
2.3.2 Residual gas analysis	25
2.4 Insulation	26
2.5 Conclusion	26
2.6 Outlook	27

3 Radiation protection	28
3.1 Plasma radiation	28
3.2 Radiation shielding	28
3.3 Radiation shielding design	29
3.4 Material	29
3.5 X-ray radiation and shielding	30
3.6 Microwave radiation and shielding	31
3.7 Windows	31
3.8 Conclusion	32
3.9 Outlook	32
4 Cost estimation	33
4.1 Outlook	34

Introduction

As part of the course "Fusion Reactor Design" held at *TU Graz* and *TU Munich* students have to design a table top fusion stellarator. This report focus on the design of the vacuum and the vacuum vessel. This includes the main recipient, the ports and the vacuum pumps. The report is divided into four primary sections: Vacuum Chamber Design, Vacuum Design, Radiation Protection and Cost Estimation.

In the first section, we delve into the design of the vacuum chamber, detailing its structure, components, and the various ports and feedthroughs incorporated for different purposes, explaining their specific roles. The Vacuum Design section is dedicated to achieving Ultra High Vacuum (UHV) conditions using a turbomolecular pump, and it also addresses the challenges of insulation and outgassing. The following section addresses the critical aspect of radiation protection, considering the various types of radiation emitted from the plasma and the design of the radiation shield. The final section, Cost Estimation, provides a detailed breakdown of the costs associated with the design and implementation of the fusion reactor. But it should be noted that not all the costs, especially the price of the the entire vacuum chamber is not included, as most of the components are not commercially available and have to be custom made.

This report is a collaborative effort by a team, each contributing their expertise to different sections of the report and also provides an overview of the ports required by each team involved in the design process, including the vacuum team, coil team, design team, diagnostic team, and heating team.

The goal of this report is to provide a detailed description of the vacuum system and rough cost estimation for the vacuum system.

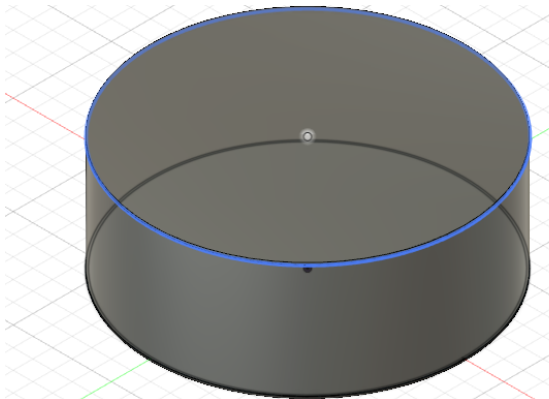
Chapter 1

Design of the vacuum chamber

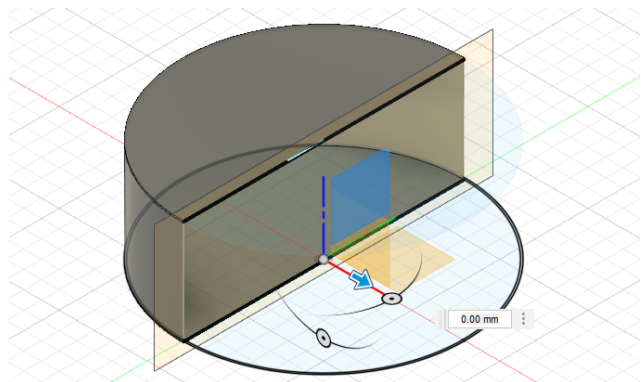
This section describes the design of the vacuum vessel, as well as the location and the dimensions of the ports. It includes our working progress of different vessel designs and the FEM simulations of the different lids. Also the different ports and feedthroughs are described in detail, for different purposes.

1.1 Main recipient

The main chamber is a simple cylinder which, including the flange, should have a size, that fits through a regular door (ca. 200 cm x 90 cm), so a volume of min. 160 cm x 60 cm was chosen for the recipient itself (see [Figure 1.1a](#)).



(a) Main recipient.



(b) Sectional analysis of the main recipient.

Figure 1.1: Main recipient.

The sectional analysis shows that the interior is naturally hollow (see [Figure 1.1b](#)), the walls, lid and base are currently 10 mm thick, although depending on the choice of central opening, the lid may be replaced by a large flange/curved top and bottom realizations with and without supporting struts. Depending on the choice of base on which the vacuum chamber will ultimately stand, consideration should also be given to possible supports for the base and lid to prevent the respective surfaces from buckling.

1.1.1 Flanges

In [Figure 1.2a](#) and [Figure 1.2b](#) the raw version of a flange and its sectional analysis is visible. There is also the possibility to assemble the flanges with the help of various libraries either from readily available parts (McMaster Carr) or to download ready-made flanges (traceparts e.g. registration required). In both cases, however, it must be known which tasks they need to fulfill.

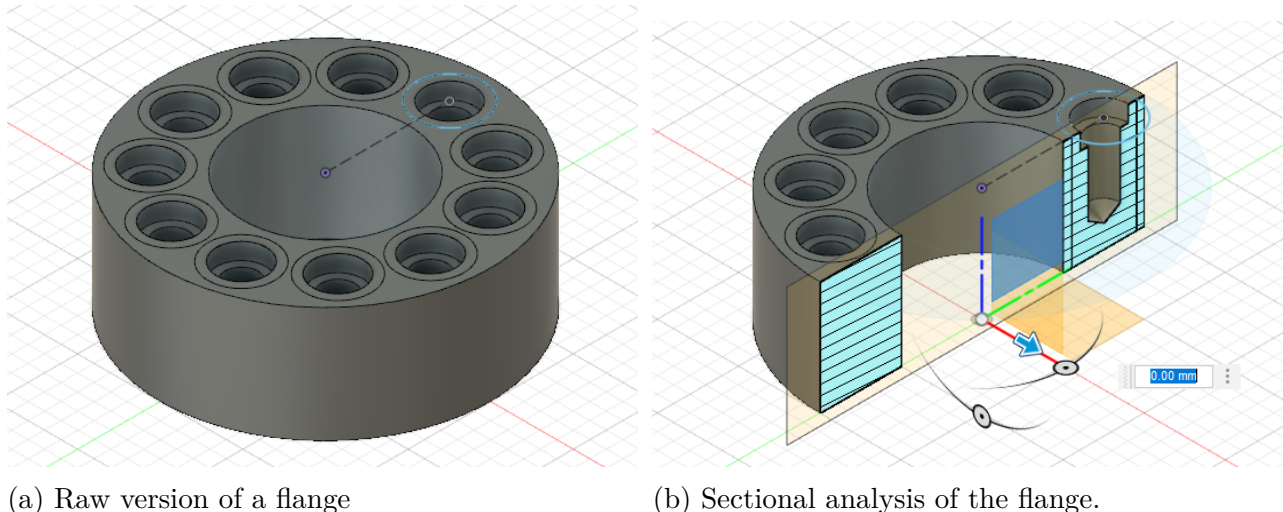


Figure 1.2: Flanges

(b) Sectional analysis of the flange.

Figure 1.2: Flanges.

1.1.2 Drill holes - options for installing windows and connections

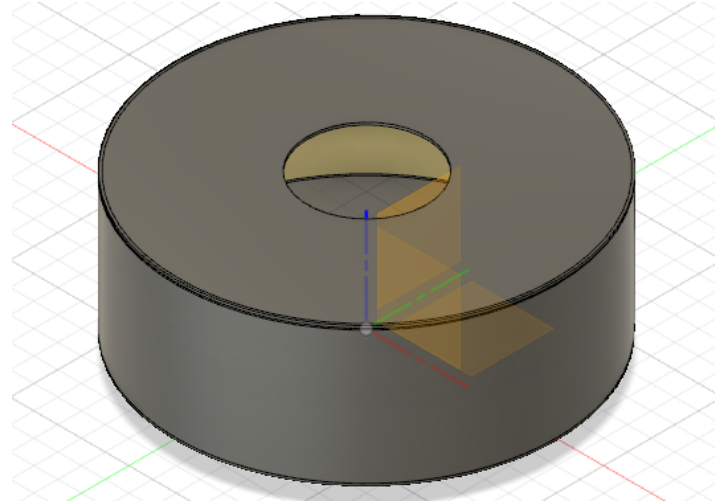


Figure 1.3: Drill hole as a possibility to realize a window in the cover.

With the help of the drilling tool, openings can be made in the existing solid body relatively easily and without complications, but once the hole has been made at a certain point, it can no longer be moved. However, it is possible to go back in time to the point at which the hole was drilled and drill it again (see [Figure 1.3](#)).

1.1.3 FEM simulations for different lid designs

The FEM simulations have shown that a domed lid on a cylindrical shell delivers the best results for stability against bending. The deformation due to the vacuum pressure is in this case max. 16 μm . The wall thickness is still 10 mm. The combination with a domed base is also possible, but involves the same difficulties as the domed lid (higher production complexity, potential customization, higher costs and special chamber support required for curved bottom). In the case of a curved lid, a thickness of 2 cm is sufficient. In addition, it would have to be considered how the entire chamber is held/stabilized and how/where the flanges of the pumps can then be attached. The inside diameter of the chamber is 160 cm and the inner height 65 cm.

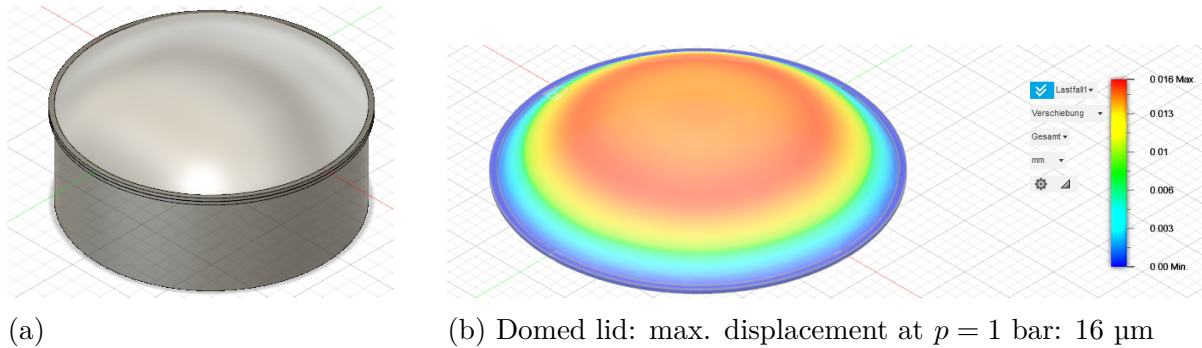


Figure 1.4: Vacuum vessel with curved lid.

The second variant would be a flat lid and base with struts. In this case, the displacements as a result of the deformations would be in the region of 100 μm , but production would probably be cheaper and simpler. One disadvantage of this design is that the large struts mean that there is less space available for potential flanges.

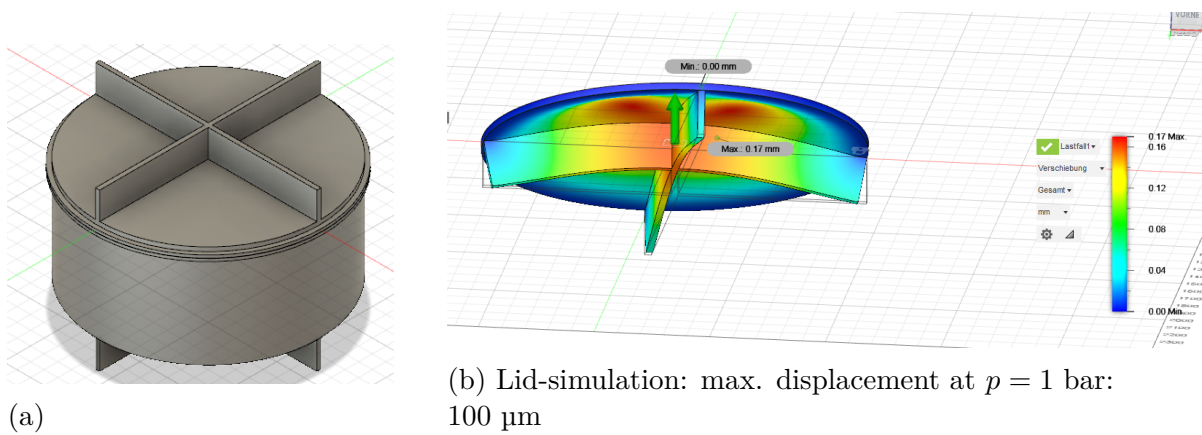


Figure 1.5: Vacuum vessel with struts.

The FEM simulation of a simple cover leads to a displacement of more than 1 mm, which is too much. The bottom plate of the chamber was chosen to be flat, with a thickness of 50 mm. This also makes it easier to attach the coils inside of the chamber, as in the case of a flat bottom, additional brackets and stabilizers for the coils could be dispensed with, as they would stand more or less on the bottom. This setup is shown in [Figure 1.6](#).

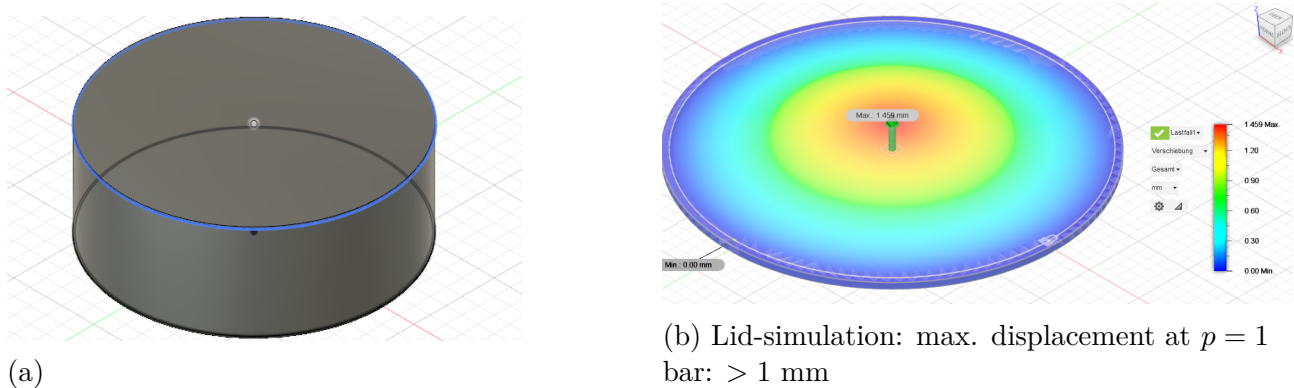


Figure 1.6: Vacuum vessel.

1.1.4 Finished design for the time being:

The various flanges are connected to the vacuum chamber step by step, starting with those of the vacuum team, as we are already familiar with them. In the meantime, some questions have arisen whose answers can be found below:

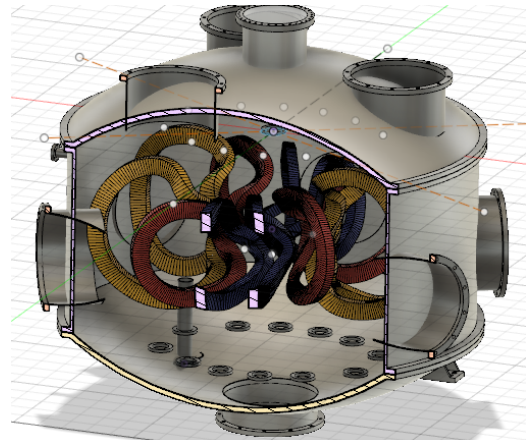
- A mirror can be moved in a vacuum chamber using piezo crystals, which should be accurate enough for the application of an interferometer.
- The position of the TMP should be chosen so that another one can be added easily and without complications. (Therefore, perhaps simply add a second flange).
- An extremely rough inner surface of the vacuum chamber would be bad, but does not really occur with stainless steel. If necessary, it can always be reground.
- The cleanliness of a vacuum chamber is very important. The best way to clean it is with a cleaning sponge (green side) and Atta (scouring agent). If necessary, follow up with isopropanol.

The shape of the vacuum chamber chosen for the time being is as visible in [Figure 1.7](#). The decision was made in favor of a curved cover and base, as this provides enough space for the coils and also best counteracts the deflection caused by the pressure difference (see [Figure 1.4b](#), the calculation of the FEM simulation results in the lowest displacement for this).

As the base of this model is also curved, as can be seen, a supporting structure is required. Possible implementations are shown at [Figure 1.8](#). The supporting structure are welded on steel lips on the side of the chamber. This lips are than placed onto steel frame outside of the chamber. Depending on how well this idea fits in with other realizations of the other four groups, it will also be added to the Fusion360 model.

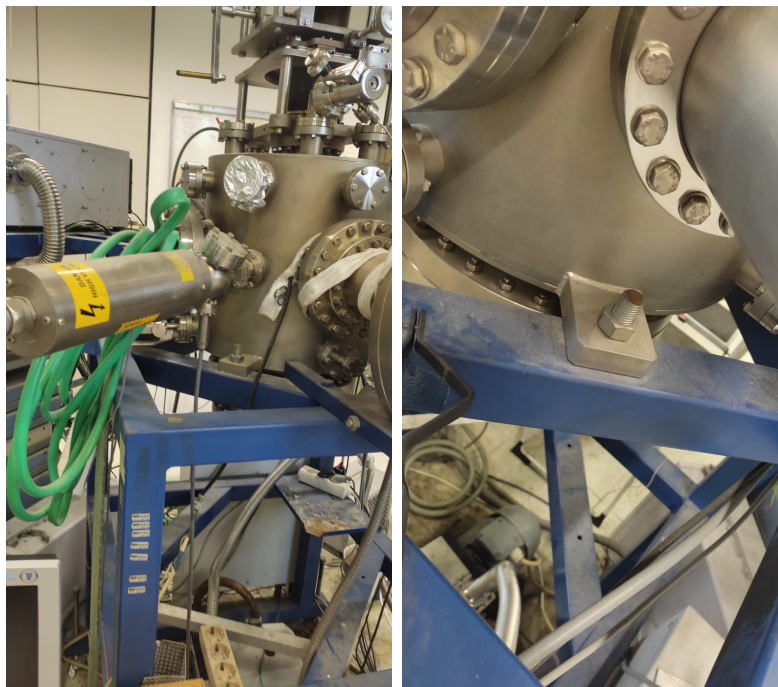


(a) Final version of the vacuum chamber.



(b) Sectional analysis of the chamber:
The flanges for the coil connections facing inwards are visible on the inside.

Figure 1.7: Views of the currently completed vacuum chamber



(a) Option to mount the vacuum chamber for the support function.

(b) Stabilizing feet for attaching the chamber to the support frame.

Figure 1.8: Possibility of stabilizing and fastening the vacuum chamber so that flange connections are possible on the floor and are freely accessible.

The mounting and the positioning of the coils inside the chamber is in the responsibility of the coil team. One need to mention that the coils should be able to be fine adjusted from the outside when the chamber is closed and evacuated. For this purpose, the coils should be mounted on ballows, which allows the movement of the coils.

1.2 Ports and feedthrough

1.2.1 (Double) o-ring gasket

To include different vacuum equipment, the components need to have a sealing surface, at which the equipment can be pressed together. A filled with elastic or plastic sealant is used due to the deviation of the ideal shape in order to make a vacuum tight connection. [36]

For the large lid a double o-ring can be used to reduce the pressure difference between the inside and the outside of the chamber. This large diamantions of the chamber make the gasket of the lid more difficult. Fortunately, the chamber is not under high pressure, so a VitonTM seal can be used. Such a gasket setup is shown in [Figure 1.9](#).

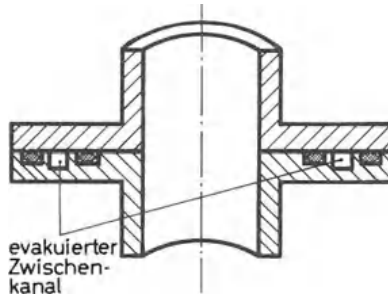
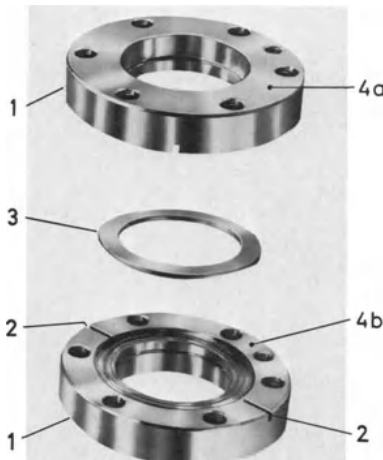


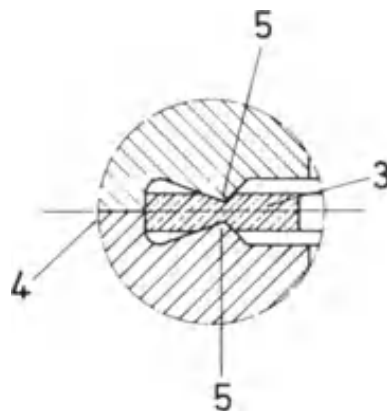
Figure 1.9: Double o-ring setup [36].

1.2.2 Copper gasket

For the smaller flanges especially when the temperature are high, a copper seal is used. The high temperature can be caused by the back out of the chamber to get a better vacuum, which out water. Thus for temperatures above 300°C a copper gasket is used, which does not outgas. For this a CF-flange is used, which is made of stainless special steel of high hardness As gasket a oxygen free copper gasket (OFHC) is used. The copper should have a hight ductility, in order to make a good seal. This sustains temperatures up to 450°C. One downside of the copper gasket is that it can only be use once, because it deforms. Thus it should be used for flanges which are not opened often.[36] A setup of a copper gasket is shown in [Figure 1.10a](#).



(a) Copper gasket with flange.



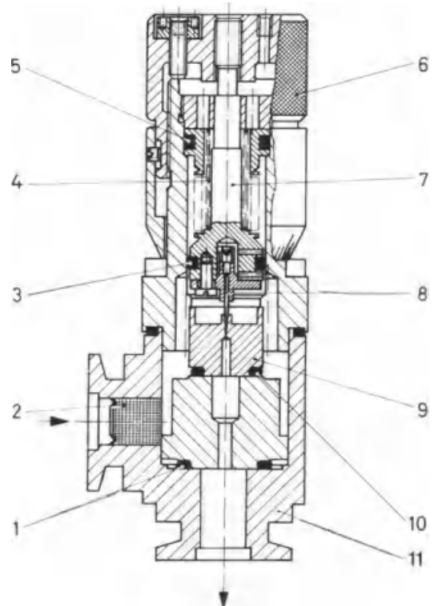
(b) Deformation of the ductile copper gasket.

Figure 1.10: Bakeable UHV flange connection with metal (Cu) seal. 1. Two identical flanges made of special stainless steel. 2. Groove for leak testing. 3. Seal disc made of OFHC copper. 4. (a, b) Flange surface with bolt circle. 5. Sealing edge, recessed relative to flange surface 4. [36].

1.2.3 Gas injection ports

To allow a controlled introduction of the gas into the vacuum chamber dosing valves are used as gas inlet ports. They are used to introduce precisely defined gas flows. The dosing valves, also known as precision valves, operate based on the principle of a needle valve and allow for a reproducible adjustment of the valve opening using a micrometer screw. The opening gap of the valve determines the gas inlet rate and measures the conductance. For commercially used dosing valves the gas inlet rates ranges from $10^{-6} \text{ cm}^3 \text{ s}^{-1}$ to $10^3 \text{ cm}^3 \text{ s}^{-1}$.

The positions of the gas inlet ports are not critical. They mainly should be positioned in such a way that the gas is evenly distributed in the chamber and efficient pumping is enabled. Since the turbomolecular pump will be positioned at the bottom of the vacuum vessel, the gas inlet ports could be positioned at the top or on the sides of the vessel [36]. In Figure 1.11 the cross-section and a real dosing valve can be seen.



(a) Cross-section of a dosing valve: 1,3,5,10 Seals with rubber-elastic material; 2 Filter in the gas (air) inlet; 4 Spring; 6 Adjustment screw - scale ring; 7 Inner part; 8 Valve needle; 9 Metal seat; 11 Housing with two small flanges. [36].

(b) Dosing valve combined with shut-off valve (without dosing drive, bottom valve drive) [36].

Figure 1.11: Dosing valve.

1.2.4 Ventilation valves

Ventilation valves, also known as vacuum relief valves, are used to control the pressure within the system. Generally, you want to place the ventilation valves in a location where one can effectively regulate the pressure throughout the chamber. An example valve from the company Pfeiffer is shown in Figure 1.12. This valve is made of stainless steel and is manually actuated. It uses a DN 10 ISO-Kf flange connection, which is a standard connection for vacuum applications.



Figure 1.12: Example ventilation valve from Pfeiffer with an DN 10 ISO-Kf fange [22].

1.2.5 Windows

Regarding windows one would have several options to choose from. The simplest solution would be **acrylic blind fanges** but they might not provide the necessary tightness or optical quality. Since these windows form a part of the vessel they replicate some essential functions of the wall. They need to be leak proof to maintain the vessel's vacuum, and they must ensure nuclear confinement. As a result, **glass windows**, some of which are plane-ground, are typically preferred. **Melted-in panes** are the only ones that can achieve extreme tightness and heat-ability. To maximize the viewing angle, the glass pane should ideally be positioned in the plane of the vessel wall. These windows can be produced with diameters up to 150 mm as standard, and the glass surface can be coated for anti-reflection or to prevent static charges. UHV viewing glasses, which need to withstand high energy doses (typically $10^6 \text{ J} \cdot \text{kg}^{-1}$ per year), must be radiation-resistant. For this purpose, either radiation-resistant types of glass or **sapphire windows** are used. The material is very resistant and can withstand high energy doses. It is more expensive than glass, but it offers excellent optical properties and high resistance to scratches and abrasion. Commonly, sapphire discs (25 mm and 50 mm) are metallized using the molybdenum-manganese method (refer to section 14.1.4) and are vacuum-sealed to a thermally adapted Ni-Fe pipe piece.[\[36\]](#) We decided to use **quartz glass**, which is also an option due to its resistance to extremely high temperatures and to radiation and its excellent transparency in UV and IR range, which can be useful for diagnostic purpose, as it allows a clear view of the plasma. Additionally it has a very low outgassing rate, therefore it won't disturb the vacuum in the Stellarator. An example window from Pfeiffer is shown in [Figure 1.13](#). This window is made of stainless steel and fused silica and uses a DN 100 CF flange connection.



Figure 1.13: Example Window from Pfeiffer with an DN 100 CF flange [\[23\]](#).

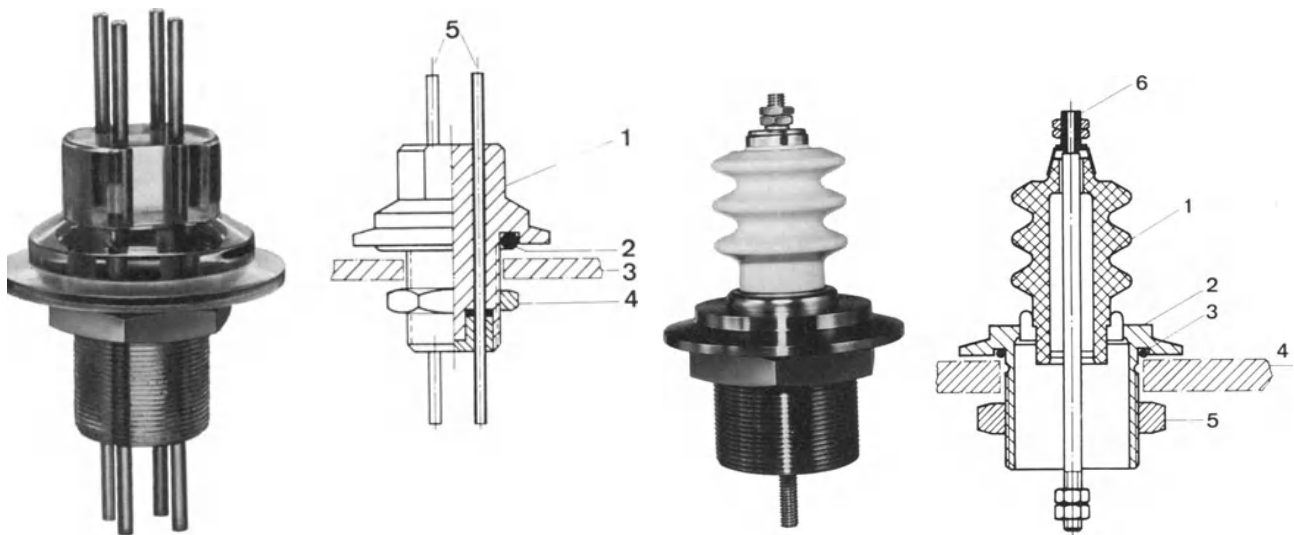
1.2.6 Sealings

For moving parts flexible spring bodies are preferably used as seals. These components can be heated higher than the other penetrations, are absolutely tight and allow a sufficient number of switching operations with the correct design. The length of these elements is determined by the required stroke. Therefore, valves with large nominal sizes are equipped with a vacuum translation to save space. In general, the sealing of the valve seat is done with a ring made of Perbunan or Viton. The tightness is sufficient for most applications. The valves can be heated up to about 150 °C when using Viton. At a working pressure below about 10^{-7} mbar, the gas release of the elastomers begins to interfere. Therefore, metal seals are used for flanges and housings. The O-ring on the valve seat is often retained even at lower pressures, as valves with all-metal sealing on the valve seat require very high forces and are particularly complex, especially in the larger diameter range [\[36\]](#).

1.2.7 Current feedthrough

As the vacuum chamber is made out of metal, the current feedthrough must be isolated to the chamber wall. For this usually plastics, glass or ceramics are used. Due to the heat expansion the connection between the chamber and the insulator must be done properly, as it causes a lot of stress on the insulator [36].

The different insulators have different temperature resistance. For low temperatures, up to $\approx 80^\circ\text{C}$, plastics can be used. For higher temperatures glass or ceramics are used. Here, one must be careful that the material of the chamber and the insulator have a similar heat expansion coefficient. Otherwise it can come to leakages or failure of the insulator [36]. A plastic insulator is shown in Figure 1.14a and a ceramic insulator in Figure 1.14b.



(a) Plastic insulator with multi current feedthrough. 1 Plastic body, designed as a small flange; 2 Rubber-elastic sealing ring; 3 Wall with hole; 4 Fastening nut; 5 Metal rods or pipes.

(b) High-voltage bushing insulated with ceramic (test voltage 25 kV). 1 Ceramic body; 2 Small flange with pipe connection; 3 Rubber-elastic seal; 4 Wall with hole; 5 Fastening nut; 6 Metal rod or metal pipe.

Figure 1.14: Current feedthrough with (a) plastic insulator and (b) ceramic insulator [36].

It should be noted that the dielectric strength is greatest for hight pressure (≈ 1 bar) and very low pressures (HV to UHV). This holdes true especially for high voltage (≈ 300 V). For pressures in between the dielectric strength is reduced, thus a electrical breakdown or a gas discharge can occur. Therefore, during evacuation and ventilation of the chamber, the voltage should be switched off [36].

1.2.8 Coaxial feedthrough



Figure 1.15: Example for a coaxial feedthrough from Pfeiffer [24].

The Grounded Shield-coaxial feedthrough features shielding potential located on the flange or welding lip. This ensures effective shielding by connecting the shield to the flange. The current rating applies per pin, and the flange material is stainless steel. The connector is designed for atmospheric conditions ranging from -65°C to 165°C . The specified voltages and currents are based on specific environmental conditions, including room temperature, dry external air, and internal vacuum of less than 10^{-4} hPa [24].

1.2.9 Cooling liquid feedthrough

When the temperature changes a lot of mechanical stress can be put on weldes and solder joints. For this case the connection between the flange and the pipe is reduced by a long and thin-walled transition piece (e.g.: a metal hose of chrome-nickel steel). The flange then retains its normal temperature, and the flowing medium is only slightly affected [36].

1.3 Manipulators (Mechanical feedthroughs)

Mechanical manipulators, also known as mechanical feedthroughs, are used to transfer movements from outside a vacuum chamber into the vacuum. They typically consist of a force-transmitting element (shaft), a seal, and a flange. These manipulators are categorized into three groups: those with dynamic seals, flexible elements, and magnetic force coupling. Manipulators with flexible elements, such as membrane or bellows, enable many precise movement types and are characterized by their lack of dynamic leakage rate. The lifespan is determined by the sizing and stress of the bellows. Manipulators with dynamic seals, such as O-ring-sealed and magnetofluid-sealed manipulators, exhibit a dynamic leakage rate between stationary and moving elements, which is typically greater than the static leakage rate. O-ring-sealed manipulators undergo continuous seal wear [14].

1.3.1 Bellows



Figure 1.16: Example for a vacuum bellow [25].

Figure 1.16 features a rotatable flange on one end and a fixed flange on the other end, allowing for flexibility in alignment and vibration resistance [25]. Bellows are used in feedthroughs with flexible elements, allowing for a wide range of precise movements. The lifespan of bellows feedthroughs is determined by the dimensioning and stress on the bellows, making proper design crucial for longevity [14].

1.3.2 Manipulator for Langmuir probe

As a manipulator for Langmuir probe one could use mechanical feedthroughs with flexible elements. These enable precise types of movement and are characterized by a low dynamic leakage rate [14].

1.3.3 Pieco motor for the interferometer mirror

One could use a vacuum-compatible Piezo linear motor actuator with Teflon-coated leads for seamless integration with vacuum-chamber feedthroughs. To ensure precise motion control and stability one could also consider the use of a closed-loop Picomotor controller and driver. This configuration, along with suitable sensor signal plug-in cards, provides the sub-nanometer resolution necessary for precise positioning and manipulation of the interferometer mirror within the vacuum chamber [1, 2].



Figure 1.17: Example for a vacuum compatible picomotor Piezo linear actuators [1].

1.4 Overview of the ports of each team

1.4.1 Vacuum - Team

Table 1.1: Overview of the ports from the **vacuum team**.

Port	Propose	Location	Type	Flange/Size
Port 1	Pirani/Bayard-Alpert manometer	outside of chamber		DN 40 CF-R
Port 2	Quadrupole mass spectrometer	outside of chamber		DN 40 CF-F
Port 3	Turbo molecular pump (TMP)	bottom		DN 320 ISO-F
Port 4	Routing pump			DN 40—50 ISO KF
Port 5	Domed lid	top		$d = 1600$ mm
Port 6	Domed bottom	bottom		$d = 1600$ mm
All other ports	any use	side and bottom		DN 320 ISO-F

For the sake of simplicity, all flange connections were chosen to have the same size. Only the connections for the Pirani-Bayard-Alpert pressure measurement and the quadrupole spectrometer were chosen differently, as little previous knowledge of specific flange sizes was known. The universal flange connections chosen for the versatile connection is the same flange used as for the TMP (cf. [Table 1.1](#)). This flange size was chosen because if a second TMP is needed, it can be easily added to the chamber using a knee. Also the relative large size of the flange allows to connect other flanges to it using adapters.

The ports for the **pumps**, especially the TMP, are planned to be located at the bottom of the chamber. As for our purpose only one TMP will be used, only one port is needed. Although, one has to keep in mind that it could make sense to add a second port for a second TMP at the bottom of the chamber, but only if there is enough space available. However, all the ports are added in such a way that there is enough space for the feet of the vacuum chamber, which carry the entire weight. Furthermore, there must be enough space under the chamber so that the length of the TMP is sufficient. The port of the roughing pump does not need to be added to the vessel itself, because it usually can be connected directly to the to TMP.

The location of the flange for the **pressure measurement** is not critical. It can be added anywhere to the chamber. One might chose the exact location when the other port locations are better known. A hot cathode tube can be used as a pressure gauge in the HV, as it does not require a magnetic field. Either a Pirani or a piezoresistive pressure transducer is suitable for the vacuum. Furthermore in [subsection 2.3.1](#).

For the residual **gas analysis** one can use a quadrupole mass spectrometer. This allows to measure the composition of the gas in the chamber. This might be useful to check if the gas which was put into the chamber was the correct one. Additionally, it helps to detect leaks in the chamber. The position of the flange for the mass spectrometer is not critical. It can be

added anywhere to the chamber. However, it is not necessary for leak detection to use a mass spectrometer attached the chamber, as there are different methods to do so. But it makes sense to include a flange for future use.

Finally, it should be mentioned that also gas inlets must be added to the chamber. They will allow a controlled introduction of the gas into the chamber. The position of these ports can be located anywhere on the chamber and it makes sense to include it last, as they do not take up much space. Thus, two or three ports can be added if necessary.

1.4.2 Coil - Team

Table 1.2: Overview of the ports from the **coil team**.

Port	Purpose	Location	Type	Flange/Size
Port	coil connection	in vicinity of actual coil position (12 coils)	-	DN 63 ISO KF

The 12 coils are connected to the vacuum chamber by using a DN 63 ISO KF flange. Each coil itself is included in a single stainless steel casing, which allows the operation of the coils in atmospheric conditions, while the chamber is evacuated. This setup excludes the coils from the vacuum, which makes it easier to run the reactor, as the cooling and power supply of the coils gets easier.

The exact positioning and mounting of the coils is in the responsibility of the coil team.

1.4.3 Design - Team

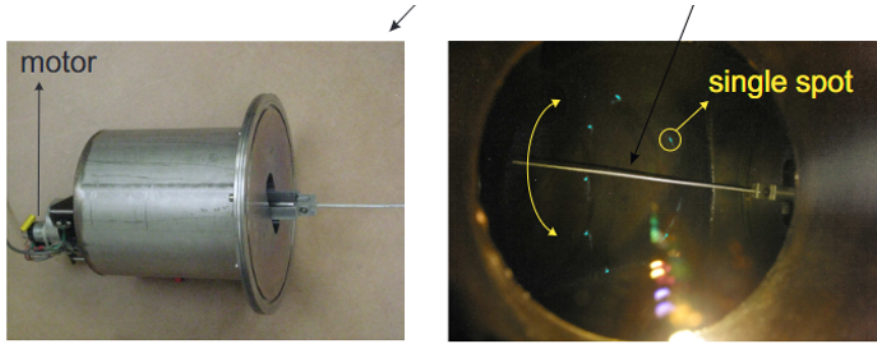
Unfortunately we did not get exact specifications nor exact definitions of their ports or locations.

1.4.4 Diagnostic - Team

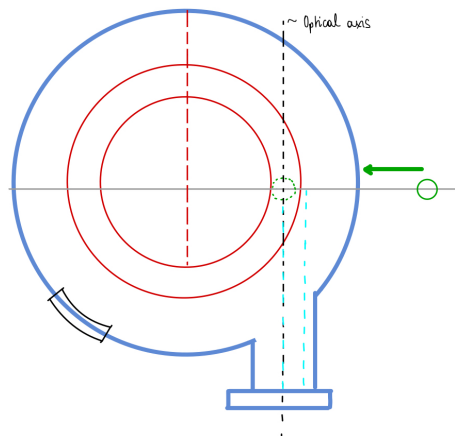
Table 1.3: Overview of the ports from the **diagnostic team**.

Port	Purpose	Location	Type	Flange/Size
Port 1	electron gun	Side (between two coils)		DN100 CF
Port 2	Window	Side (75° to Port 1)		DN400 ISO-F
Port 3	Langmuir probe / fluorescence rod	Side (between two coils)		DN400 ISO-F
Port 4 - 6	Interferometer	bottom next to the vacuum pump flange		DN320 ISO-K
Port 7	Rogowski coil	120° to each component(two diamagnetic loops and one Rogowski coil)		DN25-KF
Port 8 - 9	Diamagnetic loops	120° to each component(two diamagnetic loops and one Rogowski coil)		DN25-KF

Port 1 is the *Fluorescent rod*, its purpose is to magnetic field in the vacuum chamber. It has to be removed when the heating is started, thus it **must** be moveable. The location of this probe should be radial to the center of the chamber and the coils, respectively. An example of such a fluorescent rod is shown in [Figure 1.18a](#).



(a) Fluorescent rod in the vacuum chamber.



(b) Sketch of the fluorescent rod and the window.

Figure 1.18: Fluorescent rod.

Port 2 is the window, which is shown in the sketch [Figure 1.18a](#). The window should be positioned in a way that the surface of the rod is parallel to ones line of sight. For observation purpose, it is preferable to use quartz glass. The desired size of the window should be as large as possible, with the minimum size being determined by the inclusion of the outermost closed flux surfaces in the projection.

Port 3 is the *Langmuir probe*, its purpose is to measure the electron temperature, density and the electric potential of the plasma. The location of the probe should be on the outside of the cylinder and points towards the center of the cylinder. The size of the flange is as large as the maximum of the plasma cross-section plus ≈ 4 cm. To ensure the scanning of the entire plasma cross-section, the Langmuir probe needs to be movable in two directions. Therefore an external vacuum vessel will be utilized to house the moving components of the probe. The diameter of the probe will be 10 mm and its measuring tip 1 mm.

Port 4 includes the *Interferometer*. It need to include 2 horn antennas from the outside and a mirror on the inside, which can be adjusted in the xy-plane. The mirror need to be adjustable in the xy-plane in order to correct for the correct angle of the interferometer. To move the mirror inside of the chamber a motor is required. A sketch of the setup is shown in [Figure 1.19a](#). The horn antenna used in the interferometer is shown in [Figure 1.19b](#). Also there specific size is given.

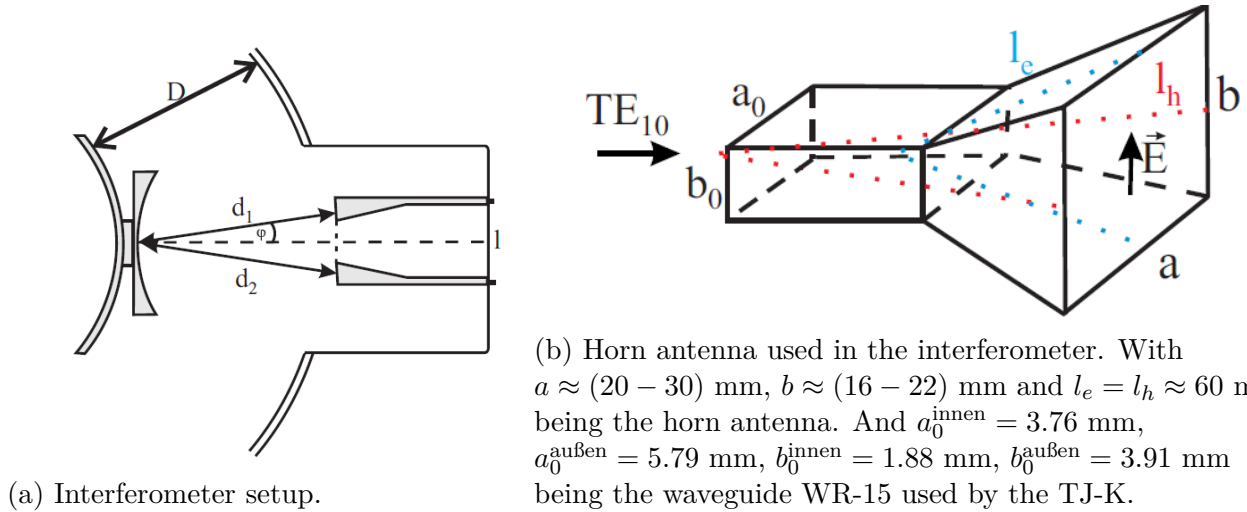


Figure 1.19: Interferometer.

Port 7 to 9 are the *Rogowski coil* and the *diamagnetic loops*. The three measurement tools need each one a coaxial cable feedthrough connections. For this a **KF-25** should be used, which is shown in [Figure 1.20a](#). The Rogowski coil and the two diamagnetic loops are spaced equally around the chamber and thus the cylindrical chamber. Therefore, a distance of $\approx 120^\circ$ is chosen between the three ports. The feedthrough are placed on the outside next to the coil and the loops, respectively. A sketch of the setup is shown in [Figure 1.20b](#).

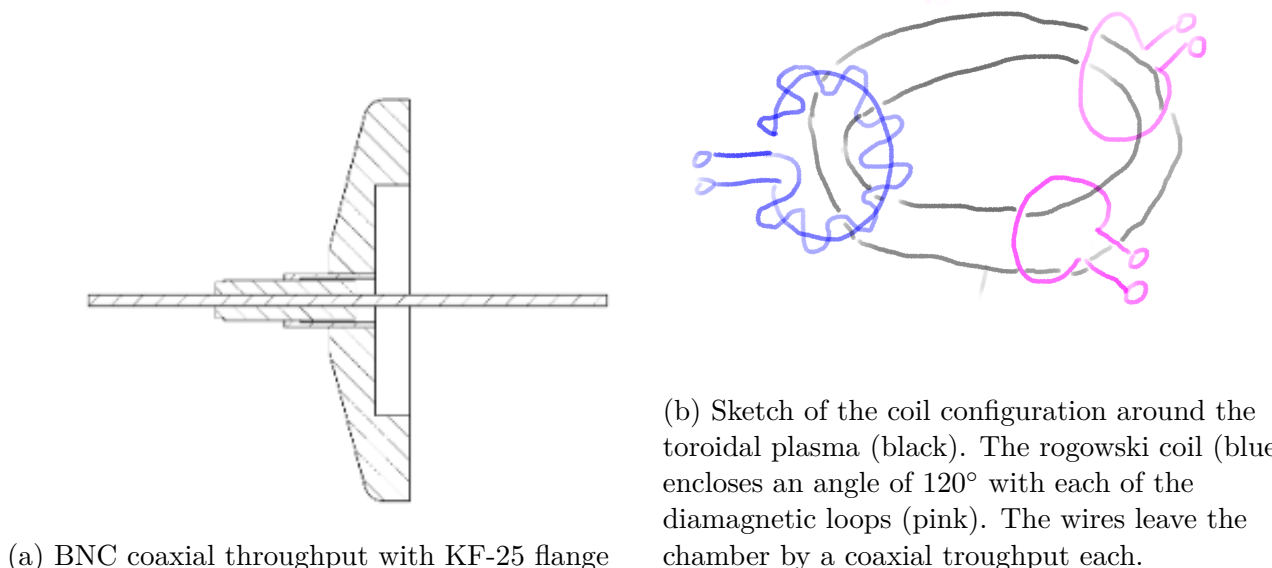


Figure 1.20: Rogowski coil and diamagnetic loops with feedthrough.

1.4.5 Heating - Team

Unfortunately we did not get exact specifications nor exact definitions of their ports or locations.

1.5 Conclusion

As mentioned in the [section 1.1](#) the process steps of the design of the main vacuum vessel is described. The first idea was to use a simple cylindrical chamber with a flat lid and base. This most simple design unfortunately did not fulfill the requirements of the vacuum chamber, as under the pressure difference of 10^{-9} mbar to atmospheric pressure, the steel lid and base would band to much. This made this design not feasible.

The second attempt was to use a supported base and a dome shaped lid. With this the bottom can be designed much more rigid and be placed easily on a palette, which has some advantages concerning transportation. The lid was designed dome shaped, which increased the rigidity a lot without increasing the thickness of the steel. This is shown in [Figure 1.4](#) and [Figure 1.6](#) for a flat and the dome shaped lid respectively.

The design of the vacuum chamber, which was finalized, is shown in [Figure 1.7](#). It has a dome shaped lid as well as a dome shaped base. This allowed to increase the size of the chamber as the base and the lid are both removable and can be placed together inside a laboratory. The given specifications of the size were given, that the chamber need to fit through a standard door, with the size of 90 cm times 200 cm.

For the sake of simplicity, the same size was chosen for all connections except for the flange for the Pirani-Bayard-Alpert pressure measurement and the one for the quadrupole spectrometer, as little previous knowledge of specific flange sizes was known. The size chosen was that of the TMP flange (see above), which has the advantage that the pump can in principle be fitted anywhere with the aid of a so-called knee. Adapters can then be installed for all other connections to ensure that any other flange size can be connected.

Apart from the ports already known for the chamber, additional ports with standard flanges are added. This makes it easier for the future use of the chamber, as retrofitting extra ports is not necessary. Also adding ports from the beginning makes it cheaper, as not much work is needed to add them later on.

1.6 Outlook

The vacuum chamber must be robust enough to withstand the pressure difference between its interior and exterior, and it must also be versatile enough to accommodate various ports and feedthroughs for different purposes. As we move forward, the design of the vacuum chamber may need to be adjusted based on the specific requirements of the other teams involved in the design process. The exact number and types of ports, as well as other components such as windows, gas inlets, feedthroughs, and coaxials, have not been finalized yet. Therefore, additional work will be needed to finalize these details and to ensure that the vacuum chamber design meets all necessary requirements. At this stage, the cost of the vacuum chamber itself remains unknown and cannot be estimated. The manufacturer does not provide list prices for such custom-made items and would only provide a cost estimate upon specific order inquiry. It is anticipated that the vacuum chamber itself would represent one of the largest expenses for the entire project, primarily due to the necessity of custom manufacturing.

Chapter 2

Vacuum design

2.1 Pressure

To model alpha-particle-like orbits with electrons one has to look at the number of toroidal rotations before collisions, which has to be comparable to the orbits of an alpha-particle heated device. Therefore, the mean free path of a moving electron has to be estimated to calculate the required pressure conditions. The mean-free path can be calculated from the temperature of the electrons $E_{kin,\beta}$ and the slowing down time τ by $l_\beta = \sqrt{2E_{kin,\beta}/m_\beta} \cdot \tau$. For a kinetic energy of $E_{kin,\beta} \approx 200$ eV and a slowing time of $\tau \approx 10$ ms the resulting mean-free path l_β equals to about 100km. In a vacuum, the electrons collide with neutrals of atomic cross-section $\sigma \approx 10^{-20}\pi m^2$ [11]. Thus the required particle density $n = 1/(l_\beta\sigma)$ is about $10^{-14} m^{-3}$. Using the ideal gas law the required pressure conditions in the vacuum vessel are in the UHV (Ultra High Vacuum) regime $< 10^{-8}$ mbar.

2.2 Pumps

In order to operate a vacuum system in UHV conditions one has to consider the gas load of the system. The gas load can be from a variety of sources, major contributions among others include initial gas contained in the system, leaks and outgassing. At UHV conditions outgassing is the largest contributor at around 90% of the total gas load [21]. For metal systems the predominant residual gas species is hydrogen. Outgassing rates can be reduced by heat treatment of the vessel and internal systems and modifying the surface of the vacuum envelope by e.g. polishing or deposition of a thin film.

The speed of a vacuum pump is defined as $S = Q/p$ with $Q = q_{p,V}$ where Q is the pumping power and p is the equilibrium pressure at the inlet. $q_{p,V}$ refers to the total gas load of the system at constant pressure and volume. Pipes and hoses which connect a vacuum pump to the chamber reduce the pumping speed S at the pump to an effective vacuum speed S_{eff} at the inlet to the chamber. For practical reasons $S \approx S_{eff}$ as the vacuum pump is directly attached to the chamber. With an estimated surface area of $15 m^2$ and an outgassing rate of $10^{-10} mbar L s^{-1} cm^{-2}$ a pumping speed of about $1700 L s^{-1}$ at $< 10^{-8}$ mbar is calculated, including other gas load contributions. This value represents just an ideal value and does not consider safety margins. The calculations correlate with the parameters of the stellarator TJ-II [30].

The vacuum pump of choice to achieve these conditions is a turbomolecular pump (TMP). A TMP consists of multiple stages of pairs of rotor and stator blades. The working principle is

that free molecules are given a momentum in a desired direction by collisions with the blades. Gas captured in the upper stages is directed to the lower stages and compressed to the level of the fore-vacuum at the outlet side. A suitable model would be the Pfeiffer Vacuum ATH3204 MT with a DN320 ISO-F inlet flange [6], which can be seen in 2.1a. The TMP is magnetically levitated, thus oil-free, and reaches a pumping speed of 3050 L s^{-1} for Nitrogen (N_2). The maximum fore vacuum of this TMP is 3 mbar, therefore an adequate backing pump has to be considered, which can transport the throughput (total gas load). The maximum gas (N_2) throughput of the ATH3204 MT is $47.5 \text{ mbar L s}^{-1}$. As the total gas load at 10^{-8} mbar is estimated at around $5 \times 10^{-5} \text{ mbar L s}^{-1}$ it is assumed that a backing pump with a pumping speed S_V of about 20 L s^{-1} is sufficient. The pumping speed of the backing pump is derived from the continuity equation $Q = p_a \cdot S_{\text{TMP}} = p_b \cdot S_V$, where p_a and p_b are the respective pressures at the inlet of the TMP and backing pump. A suitable model would be the ACP 90 from Pfeiffer vacuum, an oil-free multi-stage roots pump connected via a DN 40 hose to the TMP [4]. At the maximum possible throughput of the TMP the chosen backing pump is not capable of transporting the gas load, therefore the use case of the two pumps has to be coordinated accordingly. During operation the TMP has to be operated according to the maximum throughput of the backing pump.



(a) Turbomolecular pump: ATH3204 MT [6].



(b) Backing (Roughing) pump, multi-stage roots pump: ACP90 [4].

Figure 2.1: Vacuum system components: (a) Turbomolecular pump and (b) Backing pump.

2.3 Vacuum analysis

2.3.1 Pressure measurement

For the pressure measurement, a system containing a Pirani manometer for higher pressures and a Bayard-Alpert manometer for HV and UHV pressures would be suitable. The Pirani method uses a heating wire in a tube which is connected to the vacuum to be measured. The resistivity of the wire is temperature-dependent. As the heat convection by the gas is pressure-dependent one can measure the change in resistivity at constant voltage to determine the pressure. The gauge may be used for pressures between ATM and 10^{-4} mbar . The Bayard-Alpert gauge consists of three electrodes, a hot cathode filament, a grid and an ion collector. The filament (e.g. tungsten) emits a regulated electron current which is accelerated to the grid. Most of the

electrons collide with residual gas molecules and ionize them. The ions are attracted by the central collector and form an ion current. The ion current is proportional to the molecular gas pressure. Measurement solutions like the Pfeiffer Vacuum HPT200 [26] and the Inficon Trigon models [7] are able to measure from ATM to 5×10^{-10} mbar using just one flange.

In the Fusion360 3D model, a flange was drawn for the following combination gauge, which includes both the Pirani and the Bayard-Alpert gauge [Figure 2.2](#). All information worth knowing that guarantees the suitability of the device for the requirements at hand can be found in [Figure 2.2b](#).



Accuracy of measurement in range 1	15 % (1E-8 hPa – 1E-2 hPa) 11.25 - 7.5 · 10 ⁻³ Torr 15 - 1 · 10 ⁻² mbar	Ambient temperature	0 – 50 °C 32 - 122 °F 273.15 - 323.15 K
Bakeout temperature max.	≤ 150 °C 302 °F 423.15 K	Connection flange	DN 40 CF-R
Filament	Tungsten/iridium coated with Y ₂ O ₃	Flange, material	Stainless steel
Input voltage(s)	20 – 28 V DC	Materials in contact with media	Stainless steel Glass NiFe NiCr Cu W Mo
Measurement cable length	100 m	Measuring method	Bayard-Alpert Pirani
Measuring range	5E-10 – 1E3 mbar	Output signal: Measuring range	0.774 – 10 V
Output signal: Minimum load	10 kΩ	Power consumption max.	16 W
Pressure max.	2000 mbar	Repeatability in range 1	5 % (1E-8 hPa – 1E-2 hPa) 3.75 - 7.5 · 10 ⁻³ Torr 5 - 1 · 10 ⁻² mbar
Volume	34 cm ³	Weight	0.55 kg 1.21 lb

(a)

(b)

Figure 2.2: Measurement device including Pirani- and Bayard-Alpert-gauge [13].

2.3.2 Residual gas analysis

For future purposes, a mass spectrometer can be used to analyze the residual gas for the molecules it contains. A quadrupole spectrometer was considered for this purpose [Figure 2.3](#). It consists of an ionizer (bombardment of molecules with electrons), an ion accelerator and a mass filter consisting of four metal rods [5]. The opposing rods are applied with the same potential consisting of an RF and a DC voltage. The applied voltage affects the trajectory of the accelerated ions, only ions with a certain mass-to-charge ratio, which resonate, travel through the quadrupole filter to the ion detector. A mass spectrum can be obtained by varying the applied voltage and its frequency.



Figure 2.3: Quadrupole spectrometer: QMG 250 F1, 1-100 u, open ionsource, tungsten, I/O-option, extended [28].

There are several variants of the PrismaPro series [28], more precisely 108 different detector designs of the quadrupole spectrometer, depending on the decision criteria pressure range, the associated necessary design, as well as the analytical performance (masses to be detected, resolution, detection limit and measuring speed). The device features a DN40 CF-F flange and has a quadrupole length of 14.3 cm. Precision in the mass spectrometer is directly proportional to its cost. Measurement speed influences both the signal noise and background noise. Resolution determines the separation and signal level, with unit resolution being a common standard. Choosing the smallest suitable mass range enhances sensitivity. Detection limits depend on signal strength and peak overlaps, which vary based on the detector used [28].

2.4 Insulation

As mentioned above, in UHV systems the major contributor to the total gas load is outgassing. Outgassing of materials is temperature-dependent, thus it is key to minimize heat transfer within the UHV systems. Insulation is key to minimize outgassing and maintaining thermal stability. Furthermore, it plays an important role in sealing and preventing leaks, electrical insulation ensures safe operation and integrity of the system. In UHV systems e.g. Kapton® is widely used as an insulation material for e.g. wires due to its versatility, strong dielectric properties, high-temperature resistance, low thermal outgassing and other properties.

2.5 Conclusion

For our Vacuum system a turbo-molecular pump is chosen, due to its oil-free operation and pumping speed. It is backed up by a sufficiently sized backing pump which also provides the rough vacuum before the TMP takes over. To reduce outgassing metal surfaces in the inside are polished and wires are heat and electrically isolated by using e.g. Kapton®. Pressure is measured using a pressure gauge that includes a Pirani device for lower vacuum levels and a Bayard-Alpert device for higher vacuum ranges. For a residual gas analysis, one port is reserved for hosting a quadrupole mass spectrometer. The calculations for the sizing of the vacuum pumps are based on an estimated inner surface area of the vacuum system. As the outgassing rate scales with the surface area exposed to the vacuum, thus once the vacuum

chamber configuration with all the components inside has been finalized, the total surface area has to be assessed. The outgassing rate per area used for the calculations is based on a typical value for UHV systems, modification might be necessary. The effective vacuum speed delivered by the vacuum pumps is highly dependent on the flow conduction through pipes and hoses. Therefore the sizing of the backing pump has to be modified depending on the length of the hose and on the use case of the TMP.

2.6 Outlook

To ensure a stable UHV environment, outgassing has to be minimised by treatment e.g. polishing of the inner surface of the vessel. Further measures are reducing components inside the vessel, proper heat/electrical insulation of wires and leak prevention. Depending on the factors above the sizing of the TMP might have to be reconsidered. For the backing pump the effective pumping speed due to the hose has to be taken into account when choosing the size of the pump and matching of the operating modes of the TMP and backing pump.

Chapter 3

Radiation protection

3.1 Plasma radiation

Accelerated charged particles are sources of electromagnetic radiation. When particles are accelerated within electric or magnetic fields, they emit radiation with unique properties. In plasma, different types of radiation may occur. The simplest and most inevitable of these radiation emissions is Bremsstrahlung. This is caused by binary collisions between electrons and ions which produce photons with energy comparable to the plasma temperature [20]. When external radiation fields interact with plasma, scattered radiation is produced. Charged particles moving through magnetic fields emit either cyclotron or synchrotron radiation, depending on the energy range of the particles. Radiation can also be generated by atomic processes in plasmas with impurities, called line and recombination radiation [29]. Recombination radiation occurs when a free electron is captured by an ion, resulting in the emission of a photon. This type of emission is typically in the ultraviolet (UV) to visible range for many plasmas, depending on the energy levels of the ions. Line emission instead occurs when electrons in ions transition between discrete energy levels, emitting photons at specific wavelengths. The specific lines emitted depend on the elements present in the plasma.

3.2 Radiation shielding

In general, a radiation shield must effectively balance the following aspects as well as ensure adequate protection from the radiation emissions[10]:

1. **Activation:** An activation product is a material that has been made radioactive by the process of neutron activation. Ideally a shield would be made of a material that cannot be activated. In practice, using a low-activation material like vanadium would be rather expensive. Through careful shield design, the activation of the shield can be significantly reduced.
2. **Dose:** Radiation dose is a measure of the amount of exposure to radiation. During the design and operation of a radiation facility there must be a radiation protection system that ensures that the received doses are well below the prescribed limits.
3. **Heating/Cooling:** The nuclear heating of the shield should be kept minimal to prevent excessive energy from being deposited within the shield. Where this cannot be avoided, cooling methods must be introduced.

4. **Weight:** Shield weight is not typically a concern in stationary reactor applications. However certain parts of reactors may have strict weight limits if moving or maintenance is required. For mobile shields, it is crucial that their weight is not excessive to prevent damage to the equipment used for moving them. This is particularly important for diagnostic ports.
5. **Radiation damage:** It is important to consider the level to which a shield will become damaged in the reactor application, and if this damage can not be avoided then shield replacement should be provided.

For our purpose, only dose and cooling are relevant.

3.3 Radiation shielding design

There are a number of stages when designing a radiation shield [27]:

1. **Study of the Primary Radiation Source:** The primary radiation source determines the materials and geometry needed for the construction of the shield. Knowledge of the spatial, angular and energetic distribution of the source is essential for any future calculation.
2. **Formulation of the Basic Shield:** Once the radiation type and energy distribution of the source particles is known, the primary shielding materials can be selected depending upon how much attenuation is required.
3. **Calculation of the Attenuation of Primary Radiations:** On the basis of the over-all system evaluation and the choice of material discussed above, approximate calculations can be performed to obtain the thicknesses required to attenuate the primary radiation.

As explained in the previous section, for our stellarator we will mainly consider Bremsstrahlung radiation, which produce photons with energy comparable to the plasma temperature. Our plasma parameters are similar to the ones in the TJ-K stellarator, thus we will be working with low-temperature plasma. Typical plasma parameters for TJ-K are:

Table 3.1: Parameters of the TJ-K plasma experiment [33].

Parameter	Value
Density	$5 \times 10^{17} \text{ m}^{-3}$
Electron temperature	10 eV
Ion temperature	1 eV
Working gases	H, D, He, Ne, Ar

3.4 Material

In the selection of materials for the vacuum vessel it is important to choose non-magnetizable substances to avoid interference with the surrounding magnetic fields. One of the best option meeting this criterion is austenitic stainless steel, specifically grades 304 and 316. Steel presents many advantages for shielding due to its different properties:

1. **Density:** With its high density, steel effectively attenuates ionizing radiation such as gamma rays and X-rays, ensuring robust protection within the vacuum vessel.
2. **Availability:** Steel is widely accessible and relatively cheaper compared to some other materials used for radiation shielding.
3. **Strength:** The inherent strength of steel ensures structural integrity, especially in applications where the shielding material also serves as a structural component.
4. **Versatility:** Steel can be easily shaped and fabricated into various forms, allowing for flexibility in design and construction of shielding structures.
5. **Vacuum compatibility:** Stainless steel is commonly used in vacuum applications due to its ability to maintain performance and integrity in vacuum environments.

3.5 X-ray radiation and shielding

X-rays radiation will come from Bremsstrahlung radiation, which is primarily dependent on the electron temperature. Thus the photons will have energies up to 10 eV. The frequency of an electromagnetic wave with an energy of 10 eV is approximately 2.4×10^{15} Hz, which lies on the UV spectrum. In fact, given the plasma parameters of stellarator TJ-K, while the plasma density is relatively high, the electron and ion temperatures are quite low for significant X-ray production.

Although significant X-ray radiation is not expected from the given plasma parameters, it is still important to have some shielding against X-rays, especially if there are any unexpected events or variations in the plasma conditions. Stainless steel is less effective than materials like lead or tungsten for x-ray shielding. However, the effectiveness of stainless steel as a shield increases with its thickness. For low-energy x-rays, a few millimeters of stainless steel might provide adequate shielding.

For a beam of mono-energetic photons, the intensity of photons transmitted across some distance x in a material can be expressed with the equation

$$I = I_0 e^{-\mu x} \quad (3.1)$$

where I_0 is the initial intensity of photons and μ is the linear attenuation coefficient. The linear attenuation coefficient describes the fraction of a radiation beam that is absorbed or scattered per unit thickness of the absorber. It is photon energy dependent[12].

Since the linear attenuation coefficient of steel 316L for 10 eV energy radiation is not provided, only estimations and comparison with already constructed devices can be made.

For the design and construction of the small modular stellarator for magnetic confinement of plasma in Costa Rica (SCR-1), the vessel material was chosen to be aluminum, with an approximated thickness of 10 mm. Although using austenitic 304L grade stainless steel was analyzed, it was discarded because of the difficulty to manufacture parts according to the device dimensions and because it increased greatly project costs[34]. The plasma parameters were electron temperature $T_e = 15$ eV and electron density $n_e = 10^{17}$ m⁻³.

At the National Research Nuclear University MEPhI in Moscow, a small educational and demonstration spherical tokamak MEPhIST is under construction. The domes of the chamber were made of AISI 321 steel sheets with an initial thickness of 2.5 mm. The rest of the chamber elements were manufactured from AISI 316 steel. The thickness of the inner cylinder was 1 mm.

The thickness of the outer cylinders was 3 mm to facilitate welding with rectangular flanges [35].

TJ-K is a stellarator which has been constructed and operated in Madrid under the name TJ-I U. In 2006, TJ-K was moved to the university of Stuttgart. Since our stellarator will have the same plasma parameters as the TJ-K stellarator, we can design our vacuum chamber in a similar manner. The vessel is made of stainless steel 316L and has a wall thickness of about 10 mm [15].

3.6 Microwave radiation and shielding

For heating the plasma we will use microwave heating system operating at frequency of 2.45 GHz. Stainless steel is also a good choice material for microwave radiation shielding due to its high conductivity.

The skin depth δ describes the ability of electromagnetic radiation (particularly microwave) to penetrate a material[9]. The skin depth is related to the resistivity ρ , magnetic permeability μ and angular frequency ω according to the equation [16]

$$\delta = \sqrt{\frac{2\rho}{\mu\omega}} \quad (3.2)$$

Stainless steel 316L has resistivity $\rho = 7.4 \times 10^{-7} \Omega \text{ m}$ [8]. The relative magnetic permeability μ_r is close to 1 (non-magnetic austenitic stainless steel). The magnetic permeability $\mu = \mu_r \cdot \mu_0$ is then $\mu \approx 4\pi \cdot 10^{-7} \text{ H m}^{-1}$, where μ_0 is vacuum magnetic permeability [31]. The skin depth obtained for our frequency is $\delta \approx 8.76 \mu\text{m}$. To achieve significant attenuation of microwaves, the material thickness should be several skin depths. Typically, a thickness of about 5 skin depths is sufficient. The final thickness t required for efficiently shield from microwave radiations is then $t \approx 43.8 \mu\text{m}$. Since our vessel will be a few millimeters thick for X-ray shielding and structural integrity, this thickness is more than sufficient for microwave radiation shielding. In fact, it is orders of magnitude greater than the calculated necessary thickness for microwaves attenuation, providing efficient protection against microwave radiation.

3.7 Windows

For our project, we decide to design the stellarator with windows to look inside the vacuum chamber. Since significant X-ray radiation is not expected from the given plasma parameters, lead glass is not necessary for our purpose. We decided for quartz glass instead. For a thin, circular plate with a clamped edge subjected to a uniform pressure difference across its faces, the maximum stress can be estimated as [19, 17, 32]:

$$\sigma_{max} = \sqrt{1 - \nu + \nu^2} \frac{3}{4} \frac{pr^2}{t^2} \quad (3.3)$$

where ν is the Poisson's ratio of the glass, p is the pressure difference, t is the thickness, r is the radius of the window.

For safe operation must be valid:

$$\sigma_{max} \leq \sigma_t \quad (3.4)$$

where σ_t is the tensile strength of the glass.

For SiO_2 (quartz glass), $\sigma_t = 50 \text{ MPa}$ and $\nu = 0.17$ [18].

For a pressure difference $p = p_{out} - p_{in} \approx p_{out} = p_{atm} = 101\,300 \text{ Pa}$ ($p_{in} \approx 10^{-8} \text{ mbar} \approx 0$) and a radius $r = 100 \text{ mm}$, we obtain a thickness of about $t \geq 3.75 \text{ mm}$.

For safety reasons, it's important to include a safety factor in the thickness calculation. A safety factor compensates for uncertainties in material properties, load estimations, and potential flaws in the material. Safety factors typically range from 1.5 to 3.0 depending on the criticality of the application and the material's reliability. For our purpose, we use a SF of about 2.7. Thus, our thickness is $t = 10 \text{ mm}$. With this thickness, the maximum stress is $\sigma_{max} \approx 7 \text{ MPa}$. This value is more than 7 times less than tensile strength of SiO_2 glasses.

3.8 Conclusion

For our vacuum vessel, we have designed it with a thickness of 10 mm, which provides adequate protection against X-ray and microwave radiation. The chosen material is austenitic stainless steel 316L. This material was selected due to its non-magnetic nature and its advantageous properties, including high strength, good availability, and overall versatility, making it an ideal choice for our application.

For the window, we designed it with a circular shape having a radius 100 mm made of quartz glass. The ideal thickness for the window is 10 mm.

3.9 Outlook

A 10 mm thickness of stainless steel 316L should generally be robust enough to withstand the vacuum pressure. However, it is important to perform a detailed structural analysis to ensure the chamber can withstand external atmospheric pressure and any mechanical stresses without significant deformation or failure. Additionally, the window's mounting and sealing must be carefully designed to prevent leaks and ensure stability. It is also necessary to ensure that the design meets relevant safety standards and regulations for vacuum systems and radiation protection. Safety features such as emergency shutdown systems and radiation monitoring should be included. For this reason, integration of various sensors and instrumentation for monitoring temperature, radiation levels and other critical parameters should be considered. Moreover, it is essential to develop safety protocols for handling and maintenance, ensuring personnel are aware of and protected from potential radiation exposure.

Chapter 4

Cost estimation

After finalizing the design of the vacuum chamber and vacuum system, a cost estimation can be made. This estimation is essential for budgeting the entire project and for securing adequate funding.

Most components of the vacuum chamber can be purchased off the shelf. Table 4.2 below lists estimated costs for various parts of the vacuum system, along with an estimated quantity N for each required part. The prices above are based on prices on the website of Pfeiffer Vacuum [3]. To see the prices one has to make an account. The prices of the devices above are estimations and depend on their configuration.

Table 4.1: Overview of the estimated costs for different parts of the vacuum system.

Part	N	Price / Part (€)	Type
ATH3204 MT	1	54 000.00	Turbo Molecular Pump
ACP90	1	16 200.00	Backing Pump
ITR 90	1	1120.00	Manometer
PrismaPro®	1	11 100.00	Mass Spectrometer
Venting valve, manually actuated, stainless steel	1	94.50	Venting Valve
Weld-on flange ring, stainless steel	1	345.00	Weld-on Flange Ring
Weld-on flange, rotatable, stainless steel	1	29.60	Welding Flange
Weld-on flange, rotatable with thread, stainless steel	1	25.60	Rotatable Welding Flange

The total estimated costs in table 4.2 amount to 83,914.70 €. However, this cost estimation is not complete. For instance, the cost of the vacuum chamber itself remains unknown and cannot be estimated at this stage. The manufacturer does not provide list prices for such custom-made items and would only provide a cost estimate upon specific order inquiry. It is anticipated that the vacuum chamber itself would represent one of the largest expenses for the entire project, primarily due to the necessity of custom manufacturing.

Furthermore, the final number and types of ports, as well as other components such as windows, gas inlets, feedthroughs, and coaxials, have not been finalized or included in the cost estimation yet. For a complete list of the components and their approximate prices, different

companies such as Pfeiffer Vacuum, Streicher Machinery, Leybold, or Edwards Vacuum (just as examples, no affiliation) could be contacted. However, as mentioned before, the exact costs will highly depend on the very final design of the vacuum system, and manufacturers are often not able to list those upon order and being provided with a fixed design. In correspondence with Streicher Machinery, only the designing of the vacuum chamber would amount to around 3000 €.

The costs can be lowered by using older vacuum systems, which are or have already been in use in different laboratories at universities, and manufacturing some parts in-house.

4.1 Outlook

In the future, the costs of the whole vacuum system could be more exactly approximated by sending the design to vacuum chamber manufacturers and receiving their quotas. For this, the design shall be finalized, since without a finished system extra costs for the design might arise (≈ 3000 € as stated before), and companies do not provide cost estimates without a realistic chance of receiving an order. All costs can be lowered by incorporating the vacuum system in an already existing system, and utilizing older, used, or gifted components. Some flanges and metal pieces might be manufactured by the university's workshop, which can further lower the costs for specialized small parts.

Table 4.2: Overview of the estimated costs for different parts of the vacuum system.

Part	Price / Part (€)	Type
ATH3204 MT	54 000.00	Turbo Molecular Pump
ACP90	16 200.00	Backing Pump
ITR 90	1120.00	Manometer
PrismaPro®	11 100.00	Mass Spectrometer
Venting valve, manually actuated, stainless steel	94.50	Venting Valve
Weld-on flange ring, stainless steel	345.00	Weld-on Flange Ring
Weld-on flange, rotatable, stainless steel	29.60	Welding Flange
Weld-on flange, rotatable with thread, stainless steel	25.60	Rotatable Welding Flange

Bibliography

- [1] 2024. URL: <https://www.newport.com/f/vacuum-picomotor-actuators>.
- [2] 2024. URL: <https://www.smaract.com/en/UHV-Piezo-Stages>.
- [3] 2024. URL: <https://www.pfeiffer-vacuum.com/global/de>.
- [4] *ACP 90, SD version, three- phase (HV), manual gas ballast.* URL: https://www.pfeiffer-vacuum.com/api/empolis/resource/environment/project1_p/documents/pfeifferSharepointProd/61856-Datasheet_V9SABSCZMR01_en.pdf.
- [5] T. Adamo. “Quadrupoles: How do they work?” In: *Traces center, University of Toronto* (2020). URL: https://www.utsc.utoronto.ca/~traceslab/PDFs/MassSpec_QuadsInfo.pdf.
- [6] *ATH 3204 MT, DN 320 ISO-F, water-cooled, heated, with integrated drive electronics.* URL: <https://www.pfeiffer-vacuum.com/global/en/shop/products/TMAAAC681101>.
- [7] *BCG 450.* URL: <https://www.inficon.com/de/produkte/vakuummessgeraete-und-controller/bcg450>.
- [8] W. Callister. *Materials Science and Engineering. An Introduction.* John Wiley & Sons, 2000.
- [9] D. D. L. Chung and Murat Ozturk. “Electromagnetic skin depth of cement paste and its thickness dependence”. In: *Journal of Building Engineering* (2022).
- [10] Andrew Davis. “Radiation Shielding of Fusion Systems”. PhD thesis. School of Physics and Astronomy, University of Birmingham, 2010.
- [11] G.F. Harrer. *Rapid Prototyping Platform for Stellarator Reactor Configurations.* Project duration: 01.01.2024 – 31.12.2025. Scientific Proposal for Enabling Research Project. Technology & Systems, Jan. 2024.
- [12] Center for Nondestructive Evaluation Iowa State University. *Half-Value Layer and Attenuation Coefficient.* URL: <https://www.nde-ed.org/Physics/X-Ray/attenuationCoef.xhtml>.
- [13] *ITR90.* URL: https://www.pfeiffer-vacuum.com/global/de/shop/products/PT_T12_366_300.
- [14] Karl Jousten, ed. *Handbuch Vakuumtechnik.* Springer Reference Technik. Springer Vieweg Wiesbaden, 2018. DOI: [10.1007/978-3-658-13386-3](https://doi.org/10.1007/978-3-658-13386-3).
- [15] Alf Kohn. “Investigation of microwave heating scenarios in the magnetically confined low-temperature plasma of the stellarator TJ-K”. PhD thesis. Institut f”ur Plasmaforschung der Universit”at Stuttgart, 2010.
- [16] George M. Kunkel. *Shielding of Electromagnetic Waves, Theory and Practice.* Springer, 2020.

- [17] L.D. Landau and E.M. Lifshitz. *Theory of Elasticity*. Butterworth-Heinemann, 1986.
- [18] *Machinable Quartz*. URL: <https://www.final-materials.com/gb/43-machinable-quartz>.
- [19] Z. Molnár1, J. Égert1, and M. Bert. “Finite Element Analysis of Glass Vacuum Windows of the “COMPASS” Tokamak in Prague”. In: *Acta Technica Jaurinensis* (2015).
- [20] Edward Morse. *Nuclear Fusion*. Springer, 2018.
- [21] Samiran Mukherjee et al. “Hydrogen outgassing and permeation in stainless steel and its reduction for UHV applications”. In: *Materials Today: Proceedings* 44 (2021). International Conference on Materials, Processing & Characterization, pp. 968–974. ISSN: 2214-7853. DOI: <https://doi.org/10.1016/j.matpr.2020.11.007>. URL: <https://www.sciencedirect.com/science/article/pii/S2214785320385795>.
- [22] Pfeiffer Vacuum. *Pfeiffer Vacuum Products - Shop Products*. Accessed: 2024-06-27. 2024. URL: <https://www.pfeiffer-vacuum.com/global/en/shop/products/d75b9798-4ae8-408d-b1fb-970fa22fa890>.
- [23] Pfeiffer Vacuum. *Pfeiffer Vacuum Products - Shop Products*. Accessed: 2024-06-27. 2024. URL: https://www.pfeiffer-vacuum.com/global/en/shop/products/420GSG100_SILICA_UV.
- [24] Pfeiffer Vacuum. *Pfeiffer Vacuum Products - Shop Products*. Accessed: 2024-07-01. 2024. URL: https://www.pfeiffer-vacuum.com/global/de/shop/products/420XBG040_4.
- [25] Pfeiffer Vacuum. *Pfeiffer Vacuum Products - Shop Products*. Accessed: 2024-07-01. 2024. URL: https://www.pfeiffer-vacuum.com/global/en/shop/products/420SFK040_160.
- [26] *Pirani/Bayard-Alpert Kombination HPT 200*. URL: https://vacuum-shop.com/shop/de_DE/category/2073476/pirani-bayard-alpert-kombination-hpt-200-5101000hpa.html#hpt-200-piranibayard-alpert.
- [27] B.T. Price. *Radiation Shielding*. Pergamon Press, 1959.
- [28] *PrismaPro*. URL: <https://www.pfeiffer-vacuum.com/global/de/shop/products/6d0f7cd8-a157-453a-802a-48eac86b4c85>.
- [29] J.J. Sanderson T.J.M. Boyd. *The Physics of Plasmas*. Cambridge University Press, 2003.
- [30] FL Tabarés, A García, and J Botija. “The vacuum system of the TJ-II stellarator”. In: *Vacuum* 45.10 (1994). Special Issue Proceedings of the 1st European Topical Conference On Hard Coatings and the II Iberian Vacuum Meeting 12-15 July 1993, Alicante, Spain, pp. 1059–1061. ISSN: 0042-207X. DOI: [https://doi.org/10.1016/0042-207X\(94\)90022-1](https://doi.org/10.1016/0042-207X(94)90022-1). URL: <https://www.sciencedirect.com/science/article/pii/0042207X94900221>.
- [31] Eite Tiesinga et al. 2022. URL: [The%202022%20CODATA%20Recommended%20Values%20of%20the%20Fundamental%20Physical%20Constants.%20Database%20developed%20by%20J.%20Baker,%20M.%20Douma,%20and%20S.%20Kotochigova.%20Available%20at%20%5Curl%7Bhttps://physics.nist.gov/constants%7D,%20National%20Institute%20of%20Standards%20and%20Technology,%20Gaithersburg](https://physics.nist.gov/Constants/7D,%20National%20Institute%20of%20Standards%20and%20Technology,%20Gaithersburg).
- [32] S. Timoshenko and S. Woinowsky-Krieger. *Theory of plates and shells*. McGraw-Hill, 1959.

- [33] Institute of Interfacial Process Engineering University of Stuttgart and Plasma Technology. *The stellarator TJ-K*. URL: <https://www.igvp.uni-stuttgart.de/en/research/plasma-dynamics-and-diagnostics/experiments/TJ-K/>.
- [34] V.I. Vargas et al. “Progress on small modular stellarator SCR-1”. In: *42nd EPS Conference on Plasma Physics* (2015).
- [35] G. M. Vorobyova et al. “Vacuum Chamber of the MEPhIST-1 Tokamak”. In: *Physics of Atomic Nuclei, Vol. 83* (2020).
- [36] Max Wutz et al. *Handbuch Vakuumtechnik*. 2000. DOI: [10.1007/978-3-322-99947-4](https://doi.org/10.1007/978-3-322-99947-4).

List of Figures

1.1	Main recipient.	5
1.2	Flanges.	6
1.3	Drill hole as a possibility to realize a window in the cover.	6
1.4	Vacuum vessel with curved lid.	7
1.5	Vacuum vessel with struts.	7
1.6	Vacuum vessel.	8
1.7	Views of the currently completed vacuum chamber	9
1.8	Possibility of stabilizing and fastening the vacuum chamber so that flange connections are possible on the floor and are freely accessible.	9
1.9	Double o-ring setup [36].	10
1.10	Bakeable UHV flange connection with metal (Cu) seal. 1. Two identical flanges made of special stainless steel. 2. Groove for leak testing. 3. Seal disc made of OFHC copper. 4. (a, b) Flange surface with bolt circle. 5. Sealing edge, recessed relative to flange surface 4. [36].	11
1.11	Dosing valve.	12
1.12	Example ventilation valve from Pfeiffer with an DN 10 ISO-Kf flange [22].	12
1.13	Example Window from Pfeiffer with an DN 100 CF flange [23].	13
1.14	Current feedthrough with (a) plastic insulator and (b) ceramic insulator [36].	14
1.15	Example for a coaxial feedthrough from Pfeiffer [24].	15
1.16	Example for a vacuum bellow [25].	16
1.17	Example for a vacuum compatible picomotor Piezo linear actuators [1].	16
1.18	Fluorescent rod.	20
1.19	Interferometer.	21
1.20	Rogowski coil and diamagnetic loops with feedthrough.	21
2.1	Vacuum system components: (a) Turbomolecular pump and (b) Backing pump.	24
2.2	Measurement device including Pirani- and Bayard-Alpert-gauge [13].	25
2.3	Quadrupole spectrometer: QMG 250 F1, 1-100 u, open ionsource, tungsten, I/O-option, extended [28].	26

List of Tables

1.1	Overview of the ports from the vacuum team	17
1.2	Overview of the ports from the coil team	18
1.3	Overview of the ports from the diagnostic team	19
3.1	Parameters of the TJ-K plasma experiment [33].	29
4.1	Overview of the estimated costs for different parts of the vacuum system.	33
4.2	Overview of the estimated costs for different parts of the vacuum system.	34